

Modelling Cutting Forces using the Moduli of Elasticity in Oak Peripheral Milling

Bolesław Porankiewicz,^{a,*} Daria Wieczorek,^b Marija Djurkovic,^c Ireneusz Idzikowski,^a and Zbigniew Węgrzyn^d

This article presents an attempt to estimate the nonlinear, multivariable dependence between the main (tangential) cutting force (F_C) and the processing parameters and moduli of elasticity of oak wood (*Quercus robur*) during peripheral milling with a straight edge. The analysis indicated that the tangential force (F_C) was affected by cutting depth (c_D), feed rate per tooth (f_z), rake angle (γ_F), elastic modulus by stretching along the grain (E_{SA}), elastic modulus by stretching perpendicular to the grain (E_{SP}), elastic modulus by compression along the grain (E_{CA}), and the elastic modulus by compression perpendicular to the grain (E_{CP}). It was found that the elastic moduli (E_{SA} , E_{SP} , E_{CA} , E_{CP}) very well described the mechanical properties of processed wood. Several interactions between the examined parameters (namely, $E_{SA} \cdot \gamma_F$, $E_{SP} \cdot \gamma_F$, $E_{CP} \cdot \gamma_F$, $f_z \cdot \gamma_F$, and $f_z \cdot c_D$) were confirmed in the developed relationship $F_C = f(E_{SA}, E_{SP}, E_{CA}, E_{CP}, f_z, c_D, \gamma_F)$.

Keywords: Oak wood; Properties of wood; Machining parameters; Peripheral milling; Main cutting force

Contact information: a: Lab-Tech, Radomsko, Poland; b: Poznan University of Economics and Business, Institute of Quality Science, Department of Technology and Instrumental Analysis, al. Niepodległości 10, 61-875 Poznań, Poland; c: Department of Wood Science and Technology, University of Belgrade Faculty of Forestry, Belgrade, Serbia; d: University of Zielona Góra, Faculty of Mechanical Engineering, Institute of Mechanical Engineering, Zielona Góra, Poland; *Corresponding author: poranek@amu.edu.pl

INTRODUCTION

Throughout the years, various studies have examined the cutting process, considering wood properties and cutting conditions (Kivimaa 1950; Koch 1964; Woodson and Koch 1970; Axelsson *et al.* 1993), as well as grain orientation and wood structure (Cyra and Tanaka 1997; Goli *et al.* 2003; Porankiewicz and Goli 2014; Curti *et al.* 2019), to predict the results of machining. The calculation of the optimum values of the machining parameters could serve as the basis for predicting the behavior of the material in the machining process, the outcome of machining, and, above all, the quality of the machined surface. In general, cutting forces represent the basic parameters of the cutting process mechanics that demonstrate the basic characteristics of the cutting process conditions and behavior. The main reason for this is that the measurement of cutting forces is a powerful tool, allowing the building of physico-mechanical cutting models for a better understanding of the phenomena observed during cutting. The knowledge of the functions of cutting forces serves as the basis for ensuring a rational and economic use of means of production under the given conditions. In addition, optimization of the machining process is ensured.

There are various models in the literature that deal with the problem of calculating cutting forces. One of them is the method of coefficients (Afanasev 1961; Beršadskij 1967; Amalitskij and Lûbčenko 1977; Orlicz 1982; Goglia 1994). The aforementioned authors start from the so-called reference unit cutting resistance measured under accurately defined

conditions. Specific cutting resistances for certain materials and processing conditions are expressed as products of reference unit cutting resistances and appropriate coefficients of correction, whose values are given in adequate tables. Every change in one of the influencing parameters will also change the value of the unit cutting resistance. The principal cutting force is obtained by multiplying the calculated coefficient by the cross-sectional area of the shavings for the corresponding type of processing. The differences between the values of the forces obtained by the method of coefficients and the values of the forces measured experimentally are considerable (Mandić *et al.* 2014; Đurković and Danon 2017). One reason for such large differences is the absence of the physical and mechanical properties of the wood in the mentioned models, as they are commonly represented only by the correction coefficient for the wood species. Another reason is that the correction coefficients are not the result of a multifactorial experiment, so interdependencies between individual factors are not included in the model. There are several other possible reasons, and the conclusion would be that, to control the cutting process to achieve a sufficiently good estimate of the levels and characters of the cutting forces, the influences of the anatomical, physical, and mechanical properties of the wood should be included in the model. However, these models are usually based on extensive experiments, which are most often performed on specially designed laboratory equipment and at low cutting speeds. Therefore, they do not provide a sufficient level of generality.

There are models in the literature that include wood properties (Axelsson *et al.* 1993; Porankiewicz *et al.* 2011; Naylor *et al.* 2012; Mandić *et al.* 2015). Axelsson *et al.* (1993) gave a polynomial model equation with interactions based on multifactor experiments performed on specifically designed laboratory machines. The model includes the impacts of material properties, cutting conditions, and the angle parameter of the blades on the tangential force (F_C). The model published by Porankiewicz *et al.* (2011) was created and verified based on the experimental results of Axelsson *et al.* (1993). The model gives statistical equations for the tangential (F_C) and normal (F_N) cutting forces as functions of the physical properties of the samples, tool characteristics, and characteristics of the processing regime. Naylor *et al.* (2012) formed a model for the prediction of cutting forces and included the mechanical properties of the wood in the variables, in addition to wood density and moisture. The model published by Mandić *et al.* (2015) gives statistical equations for the main (tangential) force (F_C) as a function of the density (D), moisture content (mc), Brinell hardness (H), bending strength (R_B), the modulus of elasticity (E), feed rate per tooth (f_z), rake angle (γ_F), and cutting depth (c_D).

Đurković and Danon (2017) give a comparative analysis of calculated values (according to the method of coefficients and the model of Axelsson *et al.* (1993)) and measured values of cutting forces. The final conclusion is that the given models are simple to use and suitable for application if comparison is done between the impacts of some factors on the mechanics of cutting, but they are not suitable for quantification of their impacts, *i.e.*, calculations of specific values of the cutting forces. A major obstacle to comparing the available models is the incompatibility of the cutting parameters' ranges of variation and the values of fixed parameters for which the experiments were performed.

This study attempted to estimate the relationship the main (tangential) cutting force (F_C) and machining parameters (cutting depth (c_D), feed rate per edge (f_z), and rake angle (γ_F)) during peripheral milling of oak wood, as well as some mechanical properties (modulus of elasticity by stretching along the wood grain (E_{SA}), modulus of elasticity by stretching perpendicularly to the grain (E_{SP}), modulus of elasticity by compression along the wood grain (E_{CA}), and modulus of elasticity by compression perpendicularly to the

grain (E_{CP}). The other parameters, including cutting edge round up radius (ρ), cutting speed (v_c), diameter of the cutter (D_c), cutter width (W_c), and the number of cutting edges (z), were kept constant.

EXPERIMENTAL

Tests were performed on pedunculate oak (*Quercus robur*). Radially cut samples without observable defects in structure and color were used to determine the physical and mechanical properties. The moduli of elasticity were tested on a Zwick Roell Z010 (Ulm, Germany) testing machine. The load range for stretching along the grain was 2000 N to 2800 N, with a loading force increase rate of 1500 N/min. The load range for stretching perpendicular to the grain was 30 N to 80 N, with a loading force increase rate of 50 N/min. The load ranges for compression along and perpendicular to the grain were 8000 N to 9000 N and 500 N to 2400 N, respectively. The loading force increase rate for compression was 1500 N/min. Ranges of applied load were chosen on base of preliminary tests, in order to be below enough destructive load, and within the proportional strain defined by Hook's law. The load increment was taken according to information from reference for similar (not the same) measuring cases (Krzysik 1975).

The minimum and maximum values of the E_{SA} , E_{SP} , E_{CA} , E_{CP} , and D_{EN} are of <1164.54 MPa; 1419.26 MPa>, <54.18 MPa; 74.31MPa>, <782.1 MPa; 866.6 MPa> and <455.7 MPa; 519.8 MPa>; <692 kg/m³; 785 kg/m³> respectively.

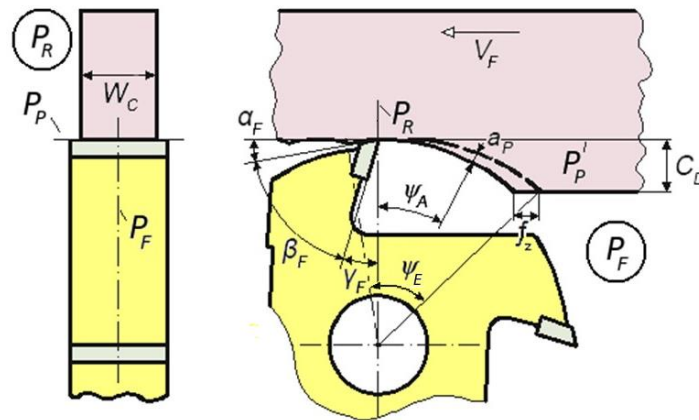


Fig. 1. Cutting situation in longitudinal milling using the cutter with a hole: a_P – average thickness of cutting layer; ψ_A – average cutter-workpiece engagement angle; ψ_E – cutter-workpiece engagement angle; P_F – working plane; P_R – main plane; P_P – back plane

Experimental research was performed using a table milling machine on a Minimax CU 410K combined machine (SCM, Rimini, Italy) equipped with a 3 kW three-phase asynchronous electrical motor (voltage 220/380 V, frequency 50 Hz, power factor 0.83) at the University of Belgrade, Faculty of Forestry Center for Machines and Apparatuses. Accessory motion was achieved using an external, removable feed device (Maggi Engineering Vario feeder, Maggi Technology, Certado, Italy), with speeds ranging between 3 m/min and 24 m/min, equipped with a 0.45 kW three-phase asynchronous electrical motor.

Testing was performed during opened, up-milling, and peripheral milling processes. The tool used consisted of three milling cutters manufactured by Freud (Straight edge cutter, Udine, Italy). The cutters were equipped with four soldered plates, made of a hard metal cemented carbide (H302). The tools were characterized by the following parameters: diameter ($D_C = 125$ mm), width ($W_C = 40$ mm (Fig.1)), radius of the round up ($\rho = 2$ μm), roughness of rake surfaces ($R_{aa} = 0.15$ μm), and roughness of clearance surfaces ($R_{ay} = 0.18$ μm). The average wood grain orientation angle toward the cutting speed velocity vector (φ_v) was in the range of 0.1241 rad to 0.1908 rad, and that toward the cutting plane (φ_s) was in the range of 0.1241 rad to 0.1908 rad. The orientation angle of the wood grain towards the cutting edge (φ_K) was 90° . Testing was performed with a constant number of rotations per minute (RPM) of the working spindle (5860 RPM, *i.e.*, at a constant cutting speed (v_c) of 38.35 m/s). Values of the other processing parameters are shown in Table 1.

Table 1. Peripheral Milling Process Parameters of Oak

Feed Speed (v_f) (m/min)	Feed Per Tooth (f_z) (mm)	Cutting Depth (c_D) (mm)	Rake Angle (γ_F) ($^\circ$)	Rake Angle (γ_F) (rad)
4	0.171	2	16	0.279
8	0.341	3	20	0.349
16	0.683	4.5	25	0.436

The cutters had a clearance angle (α_F) of 15° (Fig. 1)

The cutting power was measured indirectly, through the power input of the propulsion electric motor at each passage of the tool during the peripheral milling of the oak samples. A measuring-acquisition device (SRD1, Unolux, Belgrade, Serbia) with a sampling frequency of 100 Hz was used for data measurement, acquisition, analysis, and processing. It allowed data to be stored and displayed later (Mandić *et al.* 2015).

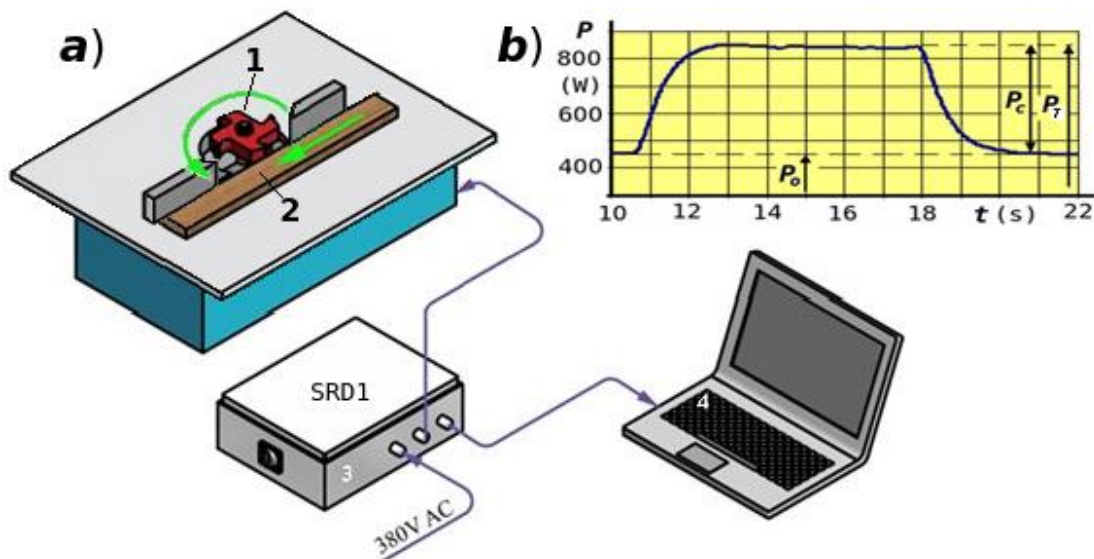


Fig. 2. (a) Experimental setup; (b) typical record of cutting power measurements during peripheral milling

Figure 2a shows the installation for cutting power recording with the following elements: (1) tool, (2) oak test sample for milling power measurement, (3) SRD1 measuring

and acquisition device, and (4) a computer configured to work with the data acquisition system. Figure 2b presents a typical record of cutting power and the manner of its processing. It is clear from the graph that the power required for cutting (P_C) is the difference between the values of total power (P_T) and power when idle (P_O) (Eq. 1).

$$P_C = P_T - P_O \quad (\text{W}) \quad (1)$$

Mean values of the main cutting force (F_A) depended on average values of the measured cutting powers (P_{CA}) (W), based on a higher number of cuts on the same test sample, and cutting speed (v_C) (m/s) (Eq. 2):

$$F_A = P_{CA} / v_C \quad (\text{N}) \quad (2)$$

The calculated value of the mean force (F_A) represents the mean force for one rotation of the tool, so it includes idle time between the blades (Fig. 3).

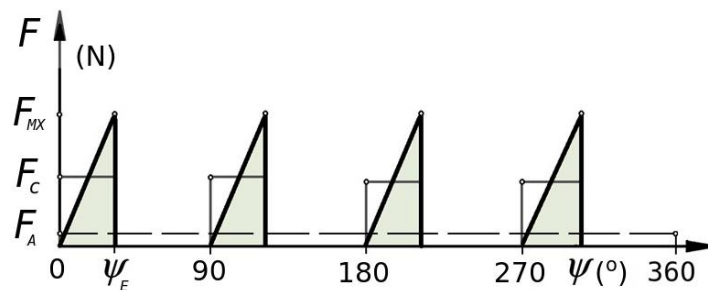


Fig. 3. Change of the main cutting force for one cutter revolution: F – tangential (main) cutting force during one revolution of the cutter; ψ – cutting edge rotation angle; ψ_E – cutting edge-workpiece engagement angle

To obtain the mean main cutting force per cutter edge (F_C), it is necessary to correct the value of the mean force (F_A) (Eq. 3),

$$F_C = 2 \cdot \pi \cdot F_A / (n \cdot \psi_E) \quad (3)$$

where F_C is the mean cutting force per blade edge (N), n is the number of milling cutter blades, and ψ_E is the cutter-workpiece engagement angle (rad) (Fig. 1).

The cutter-workpiece engagement angle can be calculated as in Eq. 4,

$$\psi_E = \arccos((R - c_D) / R) + \arcsin(f_z / (2 \cdot R)) \quad (4)$$

where R is the milling cutter radius (mm), c_D is the cutting depth (mm), and f_z is the feed rate per tooth (mm) (Fig. 1).

For each of the 22 specimens, moduli of elasticity were evaluated for a moisture content of 7%, after keeping the wood specimens in an air conditioning chamber (Wamed KBK-100, Warsaw, Poland) for 3 months. The dimensions of the cuboid wood specimens were measured using digital calipers (Kraft & Dele KD10298, Starogard Gdański, Poland): for stretching along the wood grain, 140 mm × 20 mm × 4 mm, stretching along the dimension of 140 mm; for stretching perpendicular to the wood grain, 50 mm × 10 mm × 10 mm, stretching along the dimension of 50 mm; and for compression, 20 mm × 20 mm × 30 mm, compressing along the dimension of 30 mm, along and perpendicular to the wood grain. Due to wood limitations, the specimens were not shaped exactly according to standards.

The total number of measuring points in the experimental matrix was 196. As already mentioned, the testing was conducted for various combinations of cutting process parameters. The number of repetitions for each combination of machining parameters is given in Table 2.

Table 2. Number of Repetitions for Each Combination of Machining Parameters

Feed Speed (v_F) (m/min)	4	4	.4	4	8	16	16	16	16
Cutting Depth (c_D) (mm)	2	4.5	2	4.5	3	2	4.5	2	4.5
Rake Angle (γ_F) ($^\circ$)	16	16	25	25	20	16	16	25	25
Repetitions	16	18	18	18	60	17	15	19	15

The derived values of the mean chip thickness of the cutting layer (a_P) and the angle between the cutting velocity vector (v_C) and the wood grain (ϕ_V) are given in Table 3.

Table 3. Derived Peripheral Milling Process Parameters of Oak

Feed Rate Per Tooth (f_z) (mm)	Cutting Depth (c_D) (mm)			Cutting Depth (c_D) (mm)		
	2	3	4.5	2	3	4.5
	Mean Chip Thickness of the Cutting Layer (a_P) (mm)			Angle between the Cutting Velocity Vector (v_C) and Wood Grains (ϕ_V) (rad)		
0.171	0.022	0.026	0.032	0.032	0.026	0.032
0.341	0.043	0.053	0.063	0.065	0.053	0.065
0.683	0.086	0.106	0.13	0.13	0.106	0.13

Based on the calculated average forces, the relationship $F_C = f(E_{SA}, E_{SP}, E_{CA}, E_{CP}, f_z, \gamma_F, c_D)$ was estimated in preliminary calculations for linear, polynomial, and power functions, with and without interactions. The formula should fit the experimental matrix with the lowest sum of squared residuals (S_K). This will provide the lowest standard deviation of residuals (S_R) and the highest correlation coefficient between predicted and observed values (R). The use of less complicated models will result in decreased approximation quality, with larger values of S_K and S_R and a lower R . The statistical formula determined cannot be valid outside of the ranges of independent variables chosen within the experimental matrix. With incomplete experimental matrices and complicated statistical formulas with interactions, all predicted values of the dependent variable can have greater error. Moreover, years of experience suggests that using a simple formula to fit an experimental matrix can reverse the influences of any independent variables with small importance. Only more complex mathematical formulas will ensure the correct influence of the less important independent variables. A non-linear multivariable formula with interactions (Eqs. 5 to 8) appeared to be the most appropriate in the present analysis,

$$F_C^P = a_9 \cdot e^A + B + C \quad (5)$$

where F_C^P is the predicted tangential cutting force (N), and

$$A = a_2 \cdot E_{SA} + a_3 \cdot E_{SP} + a_4 \cdot E_{CA} + a_5 \cdot E_{CP} + a_6 \cdot f_z + a_7 \cdot \gamma_F + a_8 \cdot c_D \quad (6)$$

$$B = a_{10} \cdot E_{SA} \cdot \gamma_F^{a_{16}} + a_{11} \cdot E_{SP} \cdot \gamma_F^{a_{17}} + a_{12} \cdot E_{CA} \cdot \gamma_F^{a_{18}} + a_{13} \cdot E_{CP} \cdot \gamma_F^{a_{19}} \quad (7)$$

$$C = a_{14} \cdot f_z \cdot \gamma_F^{a_{20}} + a_{15} \cdot f_z \cdot c_D^{a_{21}} + a_1 \quad (8)$$

The estimators (a_1 to a_{21}) were obtained from the 196 data points of the incomplete experimental matrix. The coefficient of relative importance (C_{RI}) (Eq. 9) was used for elimination of unimportant or low-importance estimators during the evaluation of the chosen statistical formula,

$$C_{RI} = ((S_K + S_{K0i}) / S_K) \cdot 100 \quad (\%) \quad (9)$$

where S_{K0i} is the sum of squared residuals for the estimator $a_i = 0$, where a_i is the estimator with the number i in the statistical formula evaluated.

A flow chart of the optimization program is shown in Fig. 4. For the characterization of the approximation quality, the sum of squared residuals (S_K), the standard deviation of residuals (S_R), and the correlation coefficient between the predicted and observed values (R), as well as R^2 , were applied. The calculation was performed using an optimization program based on a least squares method, combined with gradient and Monte Carlo methods (Fig. 4), at the Poznań Networking & Supercomputing Centre (PCSS) on an SGI Altix 3700 machine (Mountain View, CA, USA).

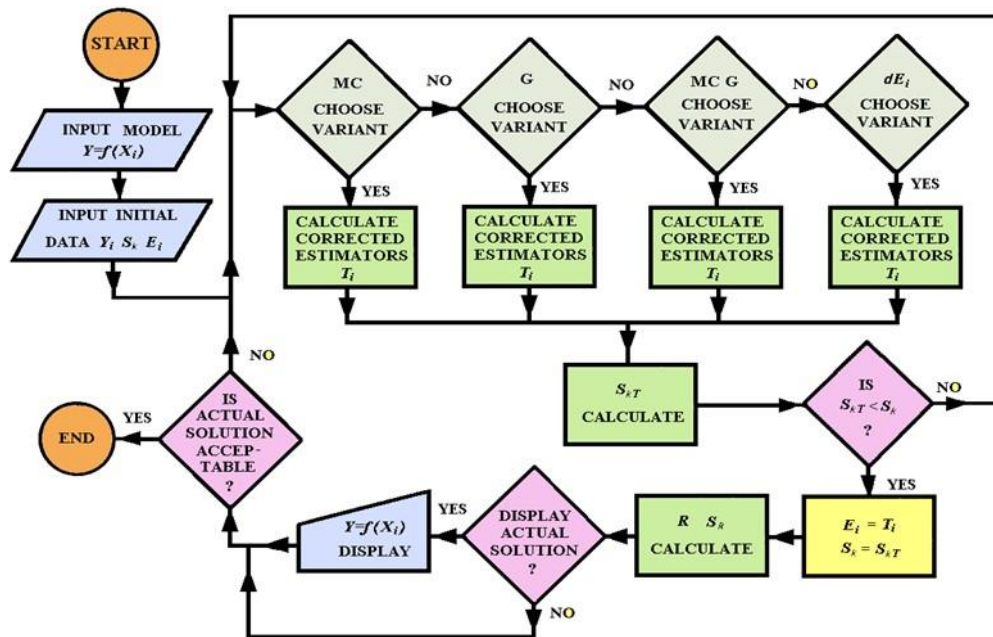


Fig. 4. Flow chart of the optimization program; variants: MC – Monte Carlo, G – gradient, MC G – combined MC and G, S_K – sum of squared residuals, R – correlation coefficient, S_R – standard deviation of residuals

RESULTS AND DISCUSSION

The final shape of the approximated dependence (Eqs. 5 to 8) was determined using the optimization program shown in Fig. 4. The following estimators were evaluated: $a_1 = 17.94648$; $a_2 = 0.025359$; $a_3 = -0.10558$; $a_4 = -0.030909$; $a_5 = 0.012781$; $a_6 = 3.61247$; $a_7 = -0.17306$; $a_8 = 0$; $a_9 = 0.0053921$; $a_{10} = -1.3162 \cdot 10^{-17}$; $a_{11} = 0$; $a_{12} = 0.11665$; $a_{13} = -24.94816$; $a_{14} = 7.8172 \cdot 10^{-17}$; $a_{15} = 1.0392 \cdot 10^{-13}$; $a_{16} = 11.070646$; $a_{17} = 0$; $a_{18} = 0$; $a_{19} = -1.81757$; $a_{20} = 12.67553$; $a_{21} = 22.40637$.

It was decided to round the estimator values to the 5 decimal (or significant) place, which produced an acceptable deterioration of the fit of less than 0.02%. Decreasing the number of rounded decimal (or significant) digits to 4, 3 and 2 caused deteriorations of the fit of as much as 3.3%, 27.9% and 1616.8%, respectively.

The coefficients of relative importance (C_{RI}) for the estimators had the following values: $C_{RI1} = 5668.3$; $C_{RI2} = 8198.7$; $C_{RI3} = 1.37 \cdot 10^{10}$; $C_{RI4} = 8.97 \cdot 10^{13}$; $C_{RI5} = 8170.5$; $C_{RI6} = 6785.9$; $C_{RI7} = 3.69 \cdot 10^6$; $C_{RI8} = 0$; $C_{RI9} = 8198.7$; $C_{RI10} = 13466.5$; $C_{RI11} = 0$; $C_{RI12} = 1.65 \cdot 10^5$; $C_{RI13} = 67744.6$; $C_{RI14} = 2475.7$; $C_{RI15} = 2683.4$; $C_{RI16} = 13466.5$; $C_{RI17} = 0$; $C_{RI18} = 0$; $C_{RI19} = 2.56 \cdot 10^9$; $C_{RI20} = 2475.7$; $C_{RI21} = 2683.4$.

For each of the 25 combinations of input data, the predicted tangential cutting force (F_C^P) was calculated using Eqs. 5 to 8. The results, together with the observed values of the main cutting force (F_C^O), are shown in Fig. 5. The approximation quality of the fit can be characterized by these quantifiers: $S_K = 1113.76$, $R = 0.994$, $R^2 = 0.987$, and $S_R = 2.39$ N. After replacing the estimators (a_1 to a_{21}) by their numerical values, Eqs. 5 to 8 take the following forms:

$$F_C^P = 0.005392 \cdot e^A + B + C \quad (10)$$

where:

$$A = 0.025359 \cdot E_{SA} - 0.10568 \cdot E_{SP} - 0.030909 \cdot E_{CA} + 0.012781 \cdot E_{CP} + 3.61247 \cdot f_z - 0.17306 \cdot \gamma_F \quad (11)$$

$$B = -1.3162 \cdot 10^{-17} \cdot E_{SA} \cdot \gamma_F^{11.070646} + 0.11665 \cdot E_{CA} - 24.94816 \cdot E_{CP} \cdot \gamma_F^{-1.81757} - 17 \quad (12)$$

$$C = 7.8172 \cdot 10^{-17} \cdot f_z \cdot \gamma_F^{12.67553} + 1.0392 \cdot 10^{-13} \cdot f_z \cdot c_D^{22.40646} + 17.94648 \quad (13)$$

Figure 5 shows that the maximum deviation from Eqs. 10 to 13 was as high as $S_R = 6.9$ N.

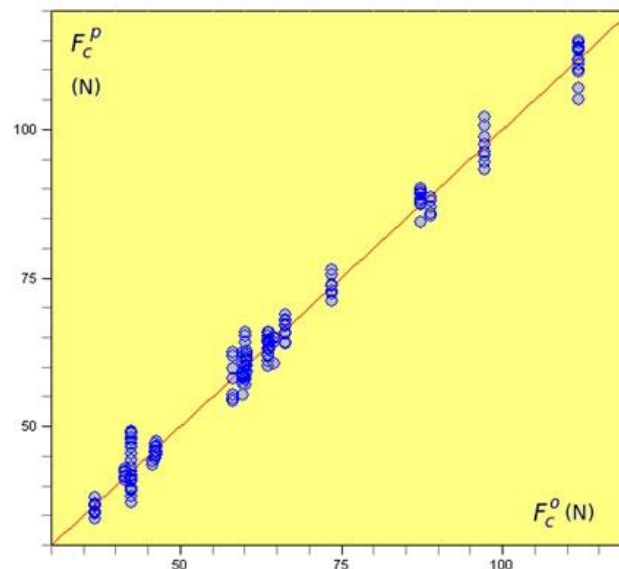


Fig. 5. Plot of the observed main force (F_C^O) and the predicted values (F_C^P), according to Eqs. 10 to 13

These equations provide a strong link between the observed cutting force (F_C^O) and the predicted cutting force (F_C^P) and can be used to analyze the influence of specific inputs on the predicted cutting forces. Equations 5 to 8 show the following interactions: $E_{SA} \cdot \gamma_F$, $E_{CP} \cdot \gamma_F$, $f_z \cdot \gamma_F$, and $f_z \cdot CD$. In the range of values of the independent variables from minimum to maximum, these interactions were changing the value of F_C^P by more than 40%. The interaction $E_{CA} \cdot \gamma_F^0$ was eliminated from Eqs. 5 to 8 during the calculation process.

Figure 6 shows the relationship of the predicted main cutting force (F_C^P) to the feed rate per tooth (f_z) and the rake angle (γ_F). As shown, F_C^P , for the largest f_z , strongly, in a parabolic increasing manner, depended on f_z . An increase in f_z increased F_C^P more at lower values of γ_F . The average change of F_C^P with an increase of the feed rate per tooth (f_z) by 0.1 mm was between 8 N and 12 N, depending on the value of the rake angle (γ_F). An increase in γ_F decreased F_C^P for the largest feed rate per tooth (f_z). As f_z decreased to less than approximately 0.6 mm, a maximum started to appear. For the lowest f_z , the influence of γ_F on F_C^P was smaller, with a maximum at a γ_F of approximately 21° . A decrease in $F_C^P = f(\gamma_F)$ for values of γ_F greater than approximately 21° is not reported in the literature.

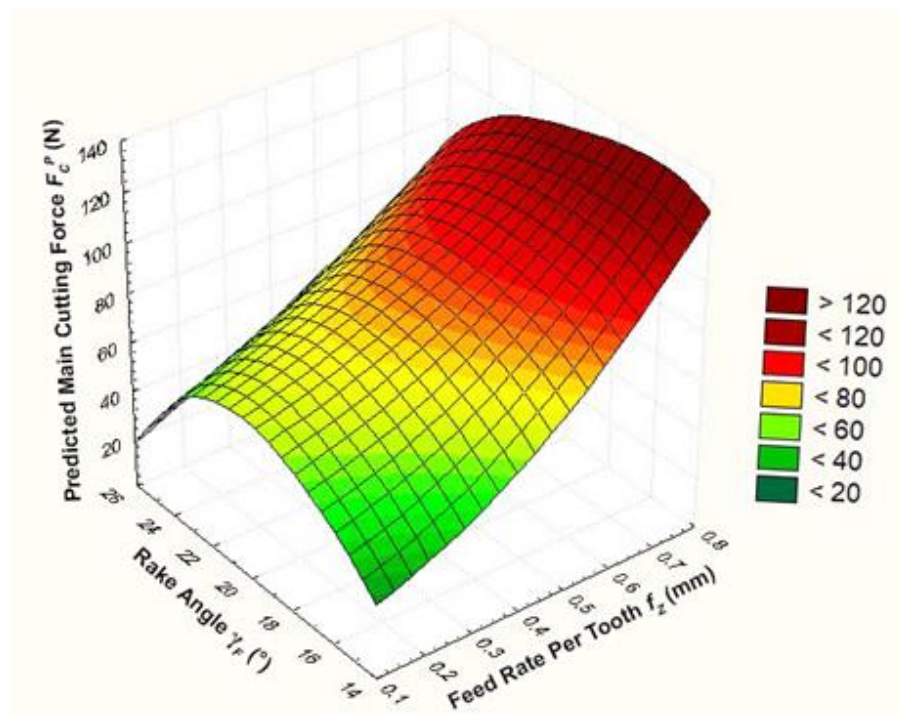


Fig. 6. Plot of the relationships among the predicted main cutting force (F_C^P) (N), γ_F ($^\circ$), and f_z (mm), according to Eqs. 10 to 13; $E_{SA} = 1419.3$ MPa; $E_{SP} = 78.11$ MPa; $E_{CA} = 882.1$ MPa; $E_{CP} = 455.7$ MPa; $CD = 4.5$ mm

Figure 7 shows the relationship of the predicted main force (F_C^P) to the moduli of elasticity (E_{SA} and E_{SP}). As shown, with an increase in E_{SA} in the range from approximately 1342 MPa to 1419.26 MPa, for a minimum $E_{SP} = 54.15$ MPa, the tangential cutting force (F_C^P) increased fast in a nonlinear, parabolic manner. For a maximum $E_{SP} = 78.1$ MPa, the tangential cutting force (F_C^P) increased much more slowly in a nonlinear, parabolic manner. The influence of the modulus of elasticity (E_{SP}) on the tangential cutting force (F_C^P) was opposite. When E_{SA} ranged from 1164 MPa to approximately 1266 MPa, F_C^P had little dependence on either E_{SA} or E_{SP} at any point in the range of variation of E_{SP} .

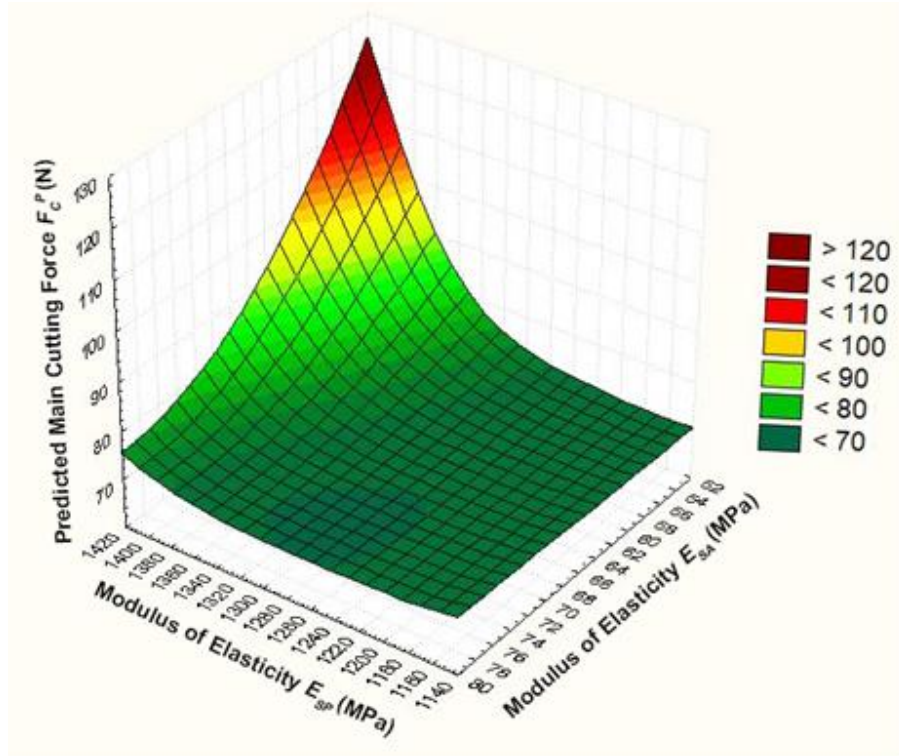


Fig. 7. Plot of the relationships among the predicted main cutting force (F_c^P) (N), E_{SA} (MPa), and E_{SP} (MPa), according to Eqs. 10 to 13; $E_{CA} = 866.6$ MPa; $E_{CP} = 519.8$ MPa; $\gamma_F = 17^\circ$; $f_z = 0.68$ mm; $c_D = 4.5$ mm

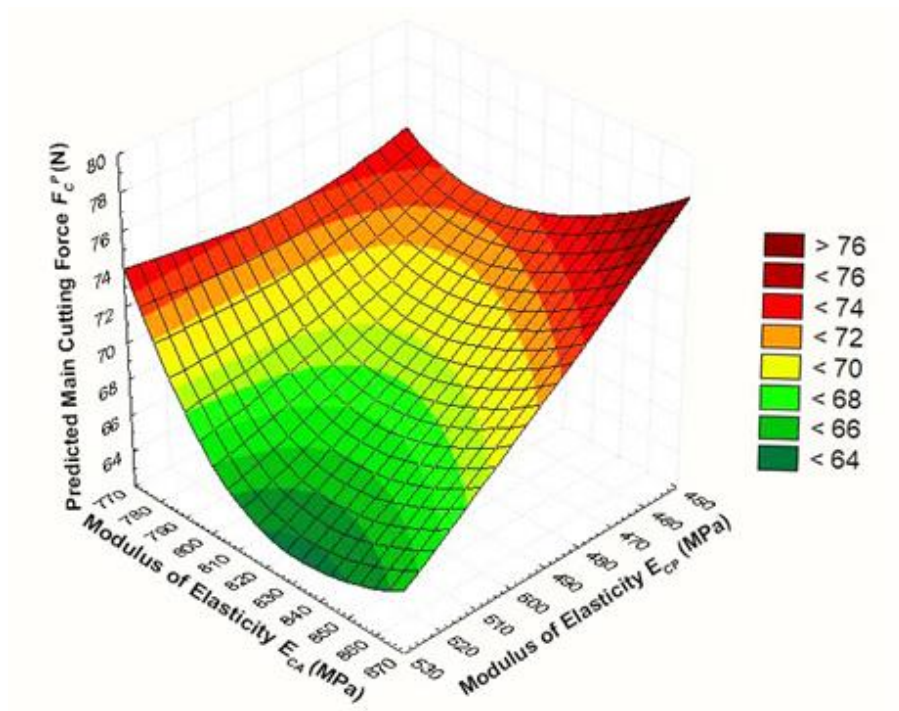


Fig. 8. Plot of the relationships among the predicted main cutting force (F_c^P) (N), E_{CA} (MPa), and E_{CP} (MPa), according to Eqs. 10 to 13; $E_{SA} = 1291.9$ MPa; $E_{SP} = 66.2$ MPa; $f_z = 0.68$ mm; $\gamma_F = 17^\circ$; $c_D = 4.5$ mm

Figure 8 shows the relationship of the predicted main cutting force (F_C^P) to the modulus of elasticity by compression along the grain (E_{CA}) and the modulus of elasticity by compression perpendicular to the grain (E_{CP}). The relationship $F_C^P = f(E_{CA})$ had a minimum between the values E_{CA} of 782.1 and 824.4 MPa, for the entire range of variation of E_{CP} . This minimum decreases and shifts for lower values of E_{CA} and E_{CP} . An increase of E_{CA} from 782.1 MPa to approximately 824.4 MPa, for the greatest $E_{CP} = 519.8$ MPa, decreased F_C^P intensively. With an increase of E_{CA} from 858 to approximately 866.6 MPa for the largest $E_{CP} = 519.8$ MPa, the predicted main cutting force (F_C^P) slightly increased. Figure 8 also shows a strong, almost linear influence of E_{CP} on the main cutting force (F_C^P) for the largest $E_{CA} = 866.6$ MPa, while the influence was much smaller for the smallest $E_{CA} = 782.1$ MPa. Based on Figs. 7 and 8, the moduli of elasticity (E_{SA} , E_{SP} , E_{CA} , and E_{CP}) of the examined oak wood described very well the main cutting force, F_C^P .

Figure 9 shows the relationship of the predicted main cutting force (F_C^P) to the cutting depth (c_D) and feed rate per tooth (f_z). As shown, c_D had a strong, non-linear influence on the main cutting force (F_C^P). The relationship $F_C^P = f(c_D)$ had a parabolic, increasing form. This relationship, especially for $c_D > 4$ mm, included the influences of a_p and, to a lesser extent, φ_V . An increase of c_D from 4 mm to 4.5 mm increased F_C^P by approximately 27.4 N. An increase in the cutting depth (c_D) from 2 mm to 4 mm changed the cutting force (F_C^P) slightly, by 2.2 N.

The analysis of the results confirmed that the examined dependency, $F_C^P = f(E_{SA}, E_{SP}, E_{CA}, E_{CP}, f_z, \gamma_F, c_D)$, was nonlinear.

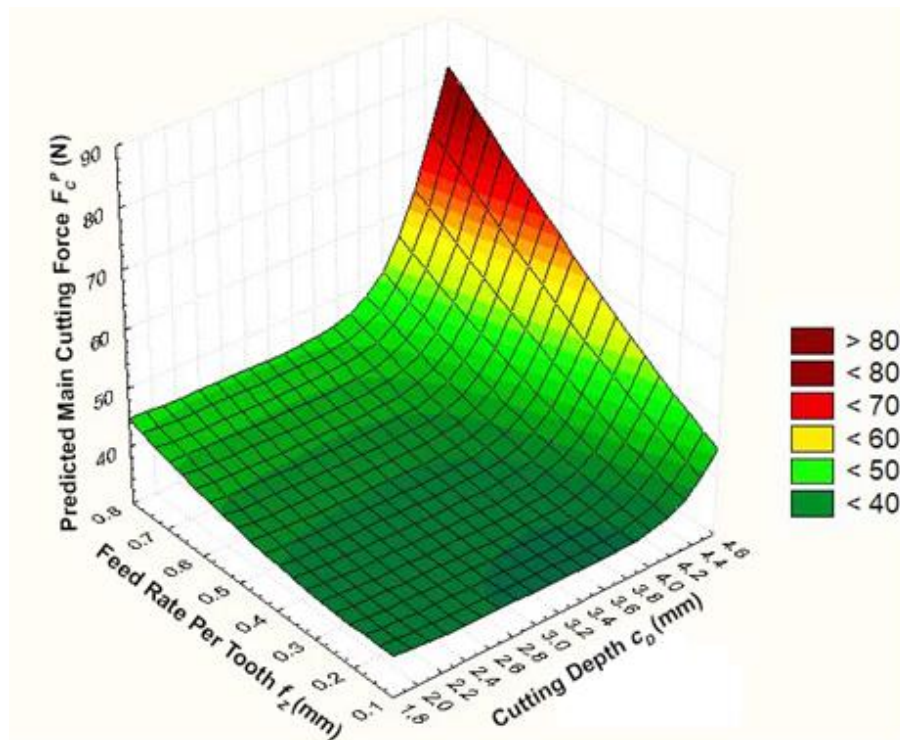


Fig. 9. Plot of the relationships among the predicted main cutting force (F_C^P) (N), feed rate per tooth (f_z) (mm), and cutting depth (c_D) (mm), according to Eqs. 10 to 13; $E_{SA} = 1291.9$ MPa; $E_{SP} = 66.2$ MPa; $E_{CA} = 782.1$ MPa; $E_{CP} = 455.7$ MPa; $\gamma_F = 16^\circ$

The main cutting force (F_C) (average in one cutting cycle) was calculated from Eqs. 10 to 13, evaluated for the following average parameters: $f_z = 0.427$ mm, $c_D = 3.25$ mm, $\gamma_F = 20.5^\circ$, $E_{SA} = 1291.9$ MPa, $E_{SP} = 66.15$ MPa, $E_{CA} = 824.4$ MPa, and $E_{CP} = 487.8$ MPa. The resulting value was $F_C = 60.14$ N. The values of F_C^P calculated from formulas published in the works Orlicz (1982), Amalitskij and Lúbčenko (1977), Beršadskij (1967), and Orlicz (1982) (f_z , c_D) were higher (19%, 3%, 65%, and 43%, respectively) than F_C^P calculated from Eqs. 10 to 13. It must be mentioned that the values of E_{SA} , E_{SP} , E_{CA} , and E_{CP} were not available in the work of Wagenführ and Scheiber (1974).

CONCLUSIONS

1. The main cutting force (F_C^P) increased in a parabolic manner with an increase of the feed rate per tooth (f_z).
2. The evaluated relationship $F_C^P = f(f_z)$ was strongest for the smallest examined rake angle ($\gamma_F = 16^\circ$).
3. The main cutting force (F_C^P), for the largest examined feed rate per tooth ($f_z = 0.7$ mm), increased in a parabolic manner with a decrease in the rake angle (γ_F). A further reduction in f_z , to the minimum of the tested values, caused a decrease of the relationship $F_C^P = f(f_z)$ and appearance of a maximum at approximately $\gamma_F \sim 21^\circ$.
4. The main cutting force (F_C^P) increased in a parabolic manner with increasing modulus of elasticity (E_{SA}), and F_C^P decreased with increasing E_{SP} .
5. The main cutting force (F_C^P) decreased in a parabolic manner with increasing modulus of elasticity (E_{SP}) and with decreasing E_{SA} .
6. The relationships $F_C^P = f(E_{SA})$ and $F_C^P = f(E_{SP})$ were very weak when E_{SA} ranged from 1150 MPa to approximately 1270 MPa.
7. In the dependence $F_C^P = f(E_{CA})$, the minimum for about $E_{CA} \sim 824$ MPa, by the largest E_{CP} was found. This minimum decreases as well as shifts for lower E_{CA} and E_{CP} values.
8. The dependence of F_C^P on the modulus of elasticity (E_{CP}) was almost linear and was stronger for a higher modulus of elasticity (E_{CA}).
9. An increase in the cutting depth (c_D) increased the main cutting force (F_C^P) in a parabolic increasing, manner, mainly when c_D ranged from 4 mm to 4.5 mm.

ACKNOWLEDGMENTS

The authors are grateful for the support of the Poznań Networking & Supercomputing Center (PCSS), Poznań, Poland, for a calculation grant (No. 241). This research was realized as a part of the project Agreement for Funding Scientific Research NIO in 2020 (registration number 451-02-68 / 2020/14/2000169), financed by the Ministry of Education and Science of the Republic of Serbia.

REFERENCES CITED

- Afanasev, P. S. (1961). *Derevoobrabatyvaúšie Stanki [Woodworking Machinery]*, Lesnaâ Promyšlennost, Moscow, Russia.
- Amalitskij, V. V., and Lûbčenko, V. I. (1977). *Stanki i Instrumenty Derevoobrabatyvaúših Predpriâtij [Machinery and Tools of Woodworking Factories]*, Lesnaâ Promyšlennost, Moscow, Russia.
- Axelsson, B. O. M., Lundberg, Å. S., and Grönlund, J. A. (1993). “Studies of the main cutting force at and near a cutting edge,” *Holz als Roh- und Werkstoff* 51(1), 43-48. DOI: 10.1007/BF02615376
- Beršadskij, A. L. (1967). *Razčet Režimov Rezaniâ Drevesiny [Resolution of Modes of Wood Machining]*, Lesnaâ Promyšlennost, Moscow, Russia.
- Curti, R., Marcon, B., Furferi, R., Denaud, L., and Goli, G. (2019). “Specific cutting coefficients at different grain orientations determined during real machining operations,” in: *Proceedings of the 24th International Wood Machining Seminar*, Corvallis, OR, USA, pp. 53-62.
- Cyra, G., and Tanaka, C. (1997). “The effects of grain orientation on routing surface finish, cutting forces and acoustic emission,” in: *Proceedings of the 13th International Wood Machining Seminar*, Vancouver, Canada, pp. 323-332.
- Durković, M., and Danon, G. (2017). “Comparison of measured and calculated values of cutting forces in oak wood peripheral milling,” *Wood Research* 62(2), 293-306.
- Goglia, V. (1994). *Strojevi i Alati za Obradu Drva I [Machinery and Tools for Wood Processing I]*, University of Zagreb, Faculty of Forestry, Zagreb, Croatia.
- Goli, G., Marchal, R., Uzielli, L., and Negri, M. (2003). “Measuring cutting forces in routing wood at various grain angles – Study and comparison between up- and down-milling techniques, processing Douglas fir and oak,” in: *Proceedings of the 16th International Wood Machining Seminar*, Matsue, Japan, pp. 127-137.
- Kivimaa, E. (1950). *The Cutting Force in Woodworking* (Rep. No. 18), The State Institute for Technical Research, Helsinki, Finland.
- Koch, P. (1964). *Wood Machining Processes*, Ronald Press Co., New York, NY, USA.
- Krzysik, F. (1975). *Nauka o Drewnie [Wood Science]*, Państwowe Wydawnictwo Naukowe, Warsaw, Poland.
- Mandić, M., Mladenović, G., Tanović, Lj., and Danon, G. (2014). “The predictive model for the cutting force in peripheral milling of oak wood,” in: *Proceedings of the 12th International Conference on Maintenance and Production Engineering KODIP*, Budva, Montenegro, pp. 231-238.
- Mandić, M., Porankiewicz, B., and Danon, G. (2015). “An attempt at modelling of cutting forces in oak peripheral milling,” *BioResources* 10(3), 5489-5502. DOI: 10.15376/biores.10.3.5489-5502
- Naylor, A., Hackney, P., Perera, N., and Clahr, E. (2012). “A predictive model for the cutting force in wood machining developed using mechanical properties,” *BioResources* 7(3), 2883-2894.
- Orlicz, T. (1982). *Obróbka Drewna Narzędziami Tnącymi [Machining of Wood with Use of Cutting Tools]*, Study book, Szkoła Główna Gospodarstwa Wiejskiego (Main School Of The Rural Farm) – Akademia Rolnicza (Agricultural Academy) (SGGW-AR), Warsaw, Poland.

- Porankiewicz, B., Axelsson, B., Grönlund, A., and Marklund, B. (2011). "Main and normal cutting forces by machining wood of *Pinus sylvestris*," *BioResources* 6(4), 3687-3713. DOI: 10.15376/biores.6.4.3687-3713
- Porankiewicz, B., and Goli, G. (2014). "Cutting forces by oak and Douglas fir machining," *Maderas. Ciencia y Tecnología* 16(2), 199-216. DOI: 10.4067/S0718-221X2014005000016
- Wagenführ, R., and Scheiber, C. (1974). *Holzatlas*, VEB Fachbuchverlag, Leipzig, Germany.
- Woodson, G. E., and Koch, P. (1970). *Tool Forces and Chip Formation in Orthogonal Cutting of Loblolly Pine* (Res. Pap. SO-52), Southern Forest Experiment Station, Forest Service, U.S. Department of Agriculture, New Orleans, LA, USA.

Article submitted: September 28, 2020; Peer review completed: December 5, 2020;
Revised version received and accepted: December 30, 2020; Published: January 7, 2021.
DOI: 10.15376/biores.16.1.1424-1437